GalNAc ≫ p-aminophenyloxypiperidinyl-α-GalNAc (unpublished results). This suggests that the bulky nitroxyl moiety interfered with binding when at some distance from the immediate sugar binding site. Figure 4 depicts a composite binding model for the spin-label analogues examined in this study.

All of the *N*-acetyl-D-galactosamine binding lectins included in this study belong to the family *Leguminoseae*; *A. bracteata* and *D. biflorus* are also classified under the same subfamily *Papilionoideae*. As the primary sequences of legume lectins have become available, extensive homologies among them have become apparent. Thus, not only the determination of their ligand binding similarities but the differences among them may eventually provide insights into the physiological role of these proteins in vivo.

Registry No. Ia, 102650-31-7; Ib, 102650-32-8; II, 102650-33-9; III, 77895-27-3; IV, 102650-34-0; Me-α-GalNAc, 6082-22-0; 3-(chloroformyl)-2,2,5,5-tetramethyl-1-oxypyrrolidine, 61593-19-9; 3-carboxy-2,2,5,5-tetramethyl-1-oxypyrrolidine, 2154-68-9; 2-amino-2-deoxy-α-D-galactopyranoside, 14196-84-0; methyl 2-deoxy-2-(*p*-nitrobenzamido)-α-D-galactopyranoside, 20581-53-7; methyl 2-deoxy-2-(*p*-aminobenzamido)-α-D-galactopyranoside, 20581-55-9; 4-isothiocyanato-2,2,6,6-tetramethyl-1-oxypiperidine, 36410-81-8.

References

Allen, A. K., Neuberger, A., & Sharon, N. (1973) *Biochem. J. 131*, 155–162.

Berliner, L. J. (1978) *Methods Enzymol. 49G*, 418–480.

Brewer, C. F., Bhattacharyya, L., Brown, R. D., III, & Koenig, S. H. (1985) *Biochem. Biophys. Res. Commun. 127*, 1066–1071.

DeBoeck, H., Lis, H., van Tilbeurgh, H., Sharon, N., & Loontiens, F. G. (1984) *J. Biol. Chem. 259*, 7067–7074.

Delmotte, F. M., & Goldstein, I. J. (1980) *Eur. J. Biochem. 112*, 219–223.

Etzler, M. E., Gupta, S., & Borrebaeck, C. (1981) *J. Biol. Chem. 256*, 2367–2370.

Galbraith, W., & Goldstein, I. J. (1972) *Biochemistry 11*, 3976–3984.

Goldstein, I. J., Plessas, R. N., Kaifu, R., Murakami, K., & Berliner, L. J. (1985) *Biochemistry 24*, 823–826.

Gould, N. R., & Scheinberg, S. L. (1970) *Arch. Biochem. Biophys. 137*, 1–11.

Griffith, O. H., Dehlinger, P., & Van, P. (1974) *J. Membr. Biol. 15*, 159–192.

Hammarström, S., Murphy, L. A., Goldstein, I. J., & Etzler, M. E. (1977) *Biochemistry 16*, 2750–2755.

Hammarström, S., Hammarström, M. L., Sundblad, G., Arnarp, J., & Lönngren, J. (1982) *Proc. Natl. Acad. Sci. U.S.A. 79*, 1611–1615.

Hayes, C. E., & Goldstein, I. J. (1974) *J. Biol. Chem. 249*, 1904–1914.

Kaifu, R., & Osawa, T. (1976) *Carbohydr. Res. 52*, 179–185.

Kaifu, R., Plantefaber, L. C., & Goldstein, I. J. (1985) *Carbohydr. Res. 140*, 37–49.

Kornfeld, R., & Kornfeld, S. (1970) *J. Biol. Chem. 245*, 2536–2545.

Lotan, R., Siegelman, H. W., Lis, H., & Sharon, N. (1973) *J. Biol. Chem. 249*, 1219–1224.

Mage, R., & Dray, S. (1965) *J. Immunol. 95*, 525–535.

Murphy, L. A., & Goldstein, I. J. (1979) *Biochemistry 18*, 4999–5005.

Neuberger, A., & Wilson, B. M. (1971) *Carbohydr. Res. 17*, 89.

Plessas, N. R., & Goldstein, I. J. (1981) *Carbohydr. Res. 89*, 211–220.

Poretz, R. D., & Goldstein, I. J. (1971) *Biochem. Pharmacol. 20*, 2727–2739.

Roberts, D. D., Etzler, M. E., & Goldstein, I. J. (1982) *J. Biol. Chem. 257*, 9198–9204.

Wright, C. (1980) *J. Mol. Biol. 141*, 267–291.

Kinetic Comparison of Ricin Immunotoxins: Biricin Conjugate Has Potentiated Cytotoxicity

Jon W. Marsh* and David M. Neville, Jr.

Section of Biophysical Chemistry, Laboratory of Molecular Biology, National Institute of Mental Health, Bethesda, Maryland 20892

Received October 15, 1985; Revised Manuscript Received March 26, 1986

ABSTRACT: The plant toxin ricin was chemically coupled to an anti-Thy-1.1 antibody, and the resultant conjugates were fractionated by gel filtration. The cytotoxicity of the conjugate possessing two ricin molecules per immunoglobulin, yielding a first-order inactivation rate of protein synthesis of −0.4 log/h at 200 ng/mL, was well above that expected just from the increase in ricin per unit mass of conjugate, when compared to a conjugate possessing only one ricin per immunoglobulin. On a conjugate molar scale the biricin immunotoxin was determined to be 8 times more potent than the monoricin conjugate; thus, relative to the number of ricin molecules, the coupling of a second ricin to the immunoglobulin quadrupled the observed potency. The concentration of immunotoxin and the resultant inactivation rates of protein synthesis were found to be related through a power function. Additionally, the inactivation kinetics of these conjugates were found to be similar to those of native ricin.

The purpose in synthesizing an immunotoxin is to combine the specificity of an antibody with the cytotoxic features of a natural toxin [for review see Neville (1985)]. Clinical application of an immunotoxin would involve the selection of an antibody directed against a pathological or undesirable group of cells; however, natural toxins lack the desired specificity and will bind to and kill most desirable nontarget cells. The plant toxin ricin, a lectin with specificity for galactose-ter-

* Address correspondence to this author.

minating complex carbohydrates (Baenziger & Fiete, 1979), can be rendered nontoxic to cultured cells by the addition of lactose. When lactose was included in the incubation, a conjugate of ricin and an anti-Thy-1.1 antibody was demonstrated in this laboratory to be 10^4 times more toxic to a target Thy-1.1 mouse leukemia cell line than to cells lacking the antigen (Youle & Neville, 1982).

An alternative to the addition of lactose to prevent nonspecific cytotoxicity is the removal of one of ricin's two subunits, the binding, or B, subunit. The A subunit possesses the enzymatic activity that inactivates the eukaryotic ribosome (Olsnes et al., 1974). Ricin A chain–monoclonal antibody conjugates, while demonstrating high specificity (Krolick et al., 1980; Gilliland et al., 1980), do not have the high killing capacity of whole toxin conjugates (Youle & Neville, 1982). The significance of B-chain function in conjugates has also been shown by the potentiation of cytotoxicity of A-chain conjugates when free B chain is included in the incubation, resulting in a 5-fold increase in the inactivation rate (Youle & Neville, 1982), as well as by the finding that the toxicity of ricin internalized by an alternative receptor, the mannose 6-phosphate receptor on fibroblasts, is dependent on the galactose-binding capability (Youle et al., 1981). Decreases in binding capacity were achieved by O-acetylation of the B subunit lectin binding site.

Most of the published work concerning immunotoxins involves clinical or preclinical applications. The chemical determinants that prevent conjugates from approaching the high toxicity seen with native toxins and the biochemical mechanisms by which immunotoxins enter the cytosol remain largely unknown. Previous conjugation procedures for coupling whole ricin to the Thy-1.1 antibody utilized the reducing agent dithiothreitol to generate reactive thiol groups through partial reduction of the immunoglobulin's native disulfide bonds (Youle & Neville, 1982). Although these conjugates were highly toxic, reaching a maximal rate of protein synthesis inhibition of −0.3 log/h at 1000 ng/mL, any subsequent analysis, particularly sodium dodecyl sulfate gel electrophoresis, was difficult. Electrophoresis of the partially reduced conjugates resulted in heterogeneous banding patterns. An alternative method of introducing thiol groups with the reagent 2-iminothiolane has permitted us to more fully characterize these conjugates and thus determine structural features that affect toxicity on target cells. Previous work from this laboratory has suggested that the entry process of immunotoxins differs from that of native toxin (Youle & Neville, 1982; Esworthy & Neville, 1984). In another report (Thorpe et al., 1984), it was suggested that the ricin B-subunit function that facilitates delivery of the A chain to the cytosol is independent of galactose recognition.

This report deals with the construction of ricin–anti-Thy-1.1 antibody conjugates, their isolation as separate species, and characterization by both chemical and cell culture techniques. We find (1) a nonlinear mathematical relationship between immunotoxin concentration and the subsequent inhibition rate of cellular protein synthesis, (2) a marked potentiation of cytotoxicity when a second ricin is coupled to the antibody, and (3) supporting evidence that certain immunotoxins may utilize the toxin's normal route of entry.

Materials and Methods

Ricin D was purified as previously described (Youle & Neville, 1982) from *Ricinus communis* beans grown in Japan, kindly provided by Dr. Gunki Funatsu, Kyushu University, Fukuoka, Japan. 2-Iminothiolane and *m*-maleimidobenzoyl *N*-hydroxysuccinimide ester (MBS)[1] were obtained from Pierce Chemical. Preformed 2–16% and 4–30% acrylamide gradient gels and Sepharose 4B were from Pharmacia. High-performance liquid chromatography was accomplished on a Hewlett-Packard 1084B with a 21.5 × 600 mm TSK-G 3000 (LKB) and a 9.4 × 250 mm Zorbax GF-250 (Du Pont) gel filtration column. RPMI 1640 and leucine-free RPMI 1640 culture media were from Gibco. L-[U-^{14}C]Leucine (300 mCi/mmol) was from ICN. Centricon microconcentrators were from Amicon. Unless otherwise noted, other materials were from Aldrich.

Production of Antibodies. Anti-Thy-1.1 monoclonal antibody MRC OX7 was obtained from hybridoma cells grown as ascites in mice and purified as described (Mason & Williams, 1980).

Thiolation of Antibody with 2-Iminothiolane. The utilization of MBS to couple thiolated OX7 antibody and ricin has previously been accomplished (Youle & Neville, 1982), but optimization of the use of 2-iminothiolane to generate a defined number of thiol groups per antibody was required. 2-Iminothiolane, dissolved in 0.8 M boric acid plus NaOH or 0.1 M phosphate, pH 8.5, was added to 100 μM OX7 immunoglobulin in PBS, so that the final protein concentration was 80 μM. After 1 h at room temperature, the protein was separated from reagent on a G-25F Sephadex column equilibrated with 0.1 M phosphate, pH 8.0, and protein concentration was determined by absorbance at 280 nm ($A_{280}^{1\,cm}$ × 0.725 = mg/mL). Thiol content was determined by addition of 5,5′-dithiobis(2-nitrobenzoic acid) (DTNB) as previously described (Ellman, 1959), using the factor 13 600 M^{-1} at 410 nm.

Synthesis of Ricin–OX7 Conjugate. Conjugation was accomplished by first generating free sulfhydryl groups on the OX7 antibody with 2-iminothiolane (Traut et al., 1973; Schram & Pülffer, 1977; King et al., 1978) and then incubating with the ricin that had previously been exposed to MBS (Kitagawa & Aikawa, 1976; Liu et al., 1979). This reagent acylates amino groups through the *N*-hydroxysuccinimidyl ester and then forms a thioether by addition of a free sulfhydryl group to the maleimide double bond.

2-Iminothiolane was dissolved in 0.8 M boric acid, pH 8.5, and then added to purified antibody at 15 mg/mL in PBS. The 2-iminothiolane addition was generally $^1/_5$ of the final volume and was in 10 molar excess over the antibody. After 1 h at room temperature, the modified antibody was freed of the reagent by gel filtration on a G-25 gel filtration column equilibrated with PBS plus 1 mM EDTA, pH 6.6. MBS, dissolved in dry dimethylformamide, was added in 1–5 molar excess over ricin, and after 20 min the entire mixture was added to the modified immunoglobulin for a final ricin:antibody molar ratio of 10:1. After 2–5 h, a 100 molar excess of *N*-ethylmaleimide over immunoglobulin was added to block any residual sulfhydryl groups.

Isolation of Conjugates. Removal of uncoupled ricin and fractionation of the conjugate were accomplished by first applying the mixture to a 21.5 × 600 mm TSK-3000 gel filtration column equilibrated with 0.1 M sodium phosphate, pH 7.2. This separated most of the ricin from the immunoglobulin peaks. These conjugate peaks were then applied to a Sepharose 4B affinity column, and the bound material was

[1] Abbreviations: MBS, *m*-maleimidobenzoyl *N*-hydroxysuccinimide ester; HEPES, 4-(2-hydroxyethyl)-1-piperazineethanesulfonic acid; PBS, phosphate-buffered saline; EDTA, ethylenediaminetetraacetic acid; SDS, sodium dodecyl sulfate; Tris, tris(hydroxymethyl)aminomethane; DTNB, 5,5′-dithiobis(2-nitrobenzoic acid); DDT, dithiothreitol; BSA, bovine serum albumin.

eluted with 10 mM lactose. After concentration on Centricon 30 microconcentrators, the material was applied to a second gel filtration column (Zorbax GF 250) to remove any remaining ricin.

Acrylamide Gradient Gel Electrophoresis. Preformed 2–16% and 4–30% acrylamide gradient gels were run on a Pharmacia GE-4 apparatus. By use of the continuous buffer system of Fairbanks et al. (1971), gels were run at 100 V, constant voltage, overnight or for 5 h for the 4–30% and 2–16% acrylamide gradient gels, respectively, then fixed, and stained with Coomassie Brillant Blue R-250. High molecular weight protein standards from Bio-Rad were used.

Densitometric Scanning of Gels. To gain a crude estimate of protein concentration per band on the acrylamide gels, scanning was done on a Shimadzu CS-930 dual wavelength scanner, measuring absorbance at 570 nm. Peak areas were determined with a Shimadzu DR-2 recorder–integrator. A standard curve was done over a range 0.5–5.0 μg/band on the 2–16% acrylamide gradient gels (2.7 nm thick). Bands containing 5 μg of OX7 antibody and of ricin toxin yielded areas of 42 700 and 39 700, respectively.

Radiolabeling of Proteins. Labeling of antibody and conjugates with $Na^{125}I$ was accomplished with the lactoperoxidase method previously described (Morrison, 1980) coupled to glucose oxidase activity as provided in kit form by New England Nuclear, following the directions therein. Generally, 1 mol of iodine could be incorporated per mole of protein. Specifics are listed in the appropriate legend.

Binding Studies. The binding of radiolabeled conjugates or antibody was accomplished on cells previously incubated at 37 °C with 25 mM 2-deoxyglucose, 5 mM sodium azide in RPMI, 25 mM HEPES, pH 7.4, and 0.1% BSA for 30 min to minimize endocytosis. Iodinated conjugates or antibody was then added at various concentrations to the AKR cells at 10^6/mL. After an additional 30-min 37 °C incubation to reach steady-state binding, 50 μL of cells was layered over 350 μL of chilled RPMI–0.1% BSA plus 250 mM sucrose in a 400 mL polyethylene microtube and immediately centrifuged. The supernatant was siphoned off, and the microtube's tip was cut and counted. Nonspecific binding was defined as the label bound in the continued presence of 100 mM lactose and 10^{-5} M unlabeled OX7 antibody and expressed as a percentage of total radioactivity added to the incubation.

Protein Synthesis Assay. The effect of toxin on protein synthesis in Thy-1.1 antigen bearing AKR SL2 cells was determined by a slight modification of previously described methods (Esworthy & Neville, 1984). Typically, 10^5 cells in leucine-free RPMI 1640 medium containing 2 mM $NaHCO_3$, 25 HEPES, pH 7.4, and 0.1% BSA were added to medium containing the desired level of immunotoxin and lactose (final concentration 100 mM), so that the final volume was 0.1 mL. This was done in a 96-well round-bottom plate. After the designated time, a 1 in 10 dilution of stock L-[U-^{14}C]leucine (0.01 mCi/mL) into leucine-free RPMI was added in a 10 μL volume to the cells. After a 60-min incubation, the cells were harvested on glass-fiber filters with a Titertek cell harvester (Flow Laboratories) and then counted. All protein synthesis assay time points were done in quadruplicate. The standard deviation on all data points is listed in the appropriate figure legend. The (pseudo-) first-order protein synthesis inactivation slopes on semilog plots, for ease of computation, have been given a positive sign. Although the loss of protein synthesis in toxin-treated cells is exponential, the rate-limiting mechanism is unknown. When this exponential function is plotted on a semilog scale, first-order rate constants (with units of reciprocal time) can be derived from the slope. However, the intoxication process is not first order with respect to anything measureable, such as toxin concentration or receptor occupancy. To prevent the appearance of any undue physical/chemical picture of the process and as a matter of simplicity and convenience, we have used the slope of the semilog plots (units: logs per hour) to characterize the rate of inactivation of protein synthesis. It is the reciprocal time value required for protein synthesis to decrease 90% of the initial value, normalized to 1 h. It is not a rate constant, but more analogous to the utilization of half-lives in describing first-order decay rates. Conversion to a pseudo-first-order rate constant can be achieved by multiplying the positive value of the slope by 2.303.

Other Methods. Ricin purification, cell culturing, and protein determination were as previously described (Youle & Neville, 1980, 1982). Statistical analysis was accomplished with software written for the HP41.

Results and Discussion

Optimization of Antibody Thiolation. The generation of thiol groups on the anti-Thy-1.1 immunoglobulin OX7 was accomplished with the reagent 2-iminothiolane. Previous generation of thiol groups on this antibody was achieved with partial reduction by dithiothreitol (DTT) at 50 mM (Youle & Neville, 1982). Lower levels resulted in decreased yields. Incubation of OX7 in 50 mM DTT resulted in the generation of 10 free sulfhydryl groups (5 cystines) per immunoglobulin molecule. To determine the level of 2-iminothiolane necessary to reach this number of thiol groups, the antibody was incubated with varying levels of 2-iminothiolane under the conditions described under Materials and Methods. A relatively large molar ratio, 100:1, of reagent:IgG was found necessary to achieve the addition of 10 thiol groups per IgG. An examination of the variously modified immunoglobulins in a coupling reaction with MBS-treated ricin demonstrated the need for only one or two new thiol groups for efficient cross-linking (data not shown). Presumably, most of the cleaved disulfides generated by DTT were not then accessible to the MBS-activated ricin; whereas, most, if not all, of the 2-iminothiolane-generated thiols were reactive. A 10:1 molar ratio of the reagent:IgG, which generates one to two thiols, was then routine.

Synthesis and Isolation of Conjugates. Ricin–immunoglobulin conjugates, prepared as described under Materials and Methods, were applied to a TSK-3000 gel filtration column, and the material was eluted as shown in Figure 1A. Two fractions representing the major peak at the position of IgG elution, fraction II, and a shoulder representing heavier material, fraction I, were separately run on a Sepharose 4B affinity column to isolate immunoglobulin possessing intact galactose-binding sites of ricin. The lighter material (II) was predominantly IgG and passed through the affinity column (Figure 1B); however, the addition of 10 mM lactose did result in the elution of conjugate. The elution of the heavier material was similar (Figure 1C). While there was some excluded material, most of the protein bound and was eluted with the lactose. The material that was eluted from both affinity runs was then rerun on another sizing column to remove any remaining free ricin.

The coupling reactions were driven by the addition of excess MBS-modified ricin against a lower level of antibody. Typically, 70–80% of the immunoglobulin became conjugated; however, when conditions were varied to optimize the yield of certain species such as single ricin conjugates (one ricin per IgG molecule) or when small fractions were isolated from the

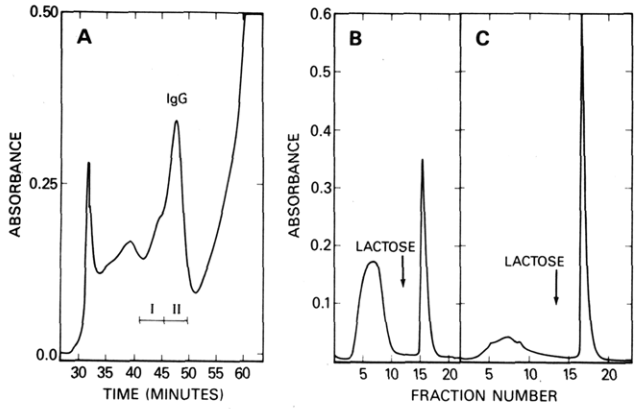

FIGURE 1: Purification of OX7–ricin immunotoxin. (A) A total of 10.5 mg of OX7 antibody was modified with 2-iminothiolane, coupled to MBS-modified ricin, as described under Materials and Methods, and applied to a 21.5 × 600 nm TSK-3000 gel filtration column. Monitoring was done at 280 nm, 0.5 AUFS. Fractions I and II were then run separately on a Sepharose 4B affinity column. (B) Affinity run of fraction II on a 10-mL bed volume column equilibrated with PBS, 4 °C. Elution of bound material was achieved by the addition of PBS plus 10 mM lactose (indicated by arrow). (C) Affinity run of fraction I, as followed by absorbance at 280 nm.

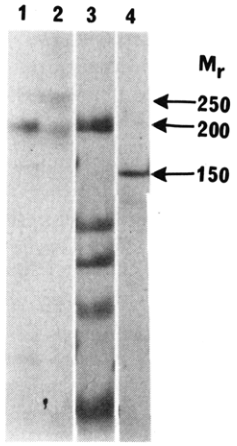

FIGURE 2: Acrylamide gradient electrophoresis gel of OX7–ricin conjugates. A linear 2–16% polyacrylamide gradient gel, using a continuous Tris–acetate buffer system, was run at 100 V, constant voltage, for 5 h, then fixed, and stained. Lane 1, 3 μg of conjugate isolated from fraction II (Figure 1A). Lane 2, 7 μg of conjugate isolated from fraction I. Lane 3, protein standards (each 2.5 μg) with molecular weights in thousands, from top to bottom: myosin (200), β-galactosidase (116.5), phosphorylase B (92.5), bovine serum albumin (66.2), and ovalbumin (45). Lane 4, 7 μg of OX7 immunoglobulin.

gel filtration step, yields were diminished. The yield of monoricin conjugate (Figure 2, lane 1) was 8% of starting immunoglobulin; the material in lane 2 was 7%. More highly purified samples resulted in decreased yields. For example, the yield of biricin conjugate (Figure 6B, lane 1) was less than 3%.

Analysis on Polyacrylamide Gradient Gels. Banding patterns on SDS–polyacrylamide gradient gels in the absence of any reducing agent showed identical patterns on either a 4–30% acrylamide gradient gel run overnight (16 h) or a 2–16% gradient gel run for 5 h. Essentially, there was one band with the purified material from peak II of the TSK-3000 column, representing an approximate molecular weight of 200 000 (Figure 2, lane 1), and two bands with the heavier conjugate preparation, peak I (see Figure 2, lane 2). One of the two bands was again at the M_r 200 000 position, whereas the higher molecular weight was approximately 250 000. This banding pattern would be consistent with an IgG–ricin conjugate possessing a one to one IgG:ricin ratio for the M_r

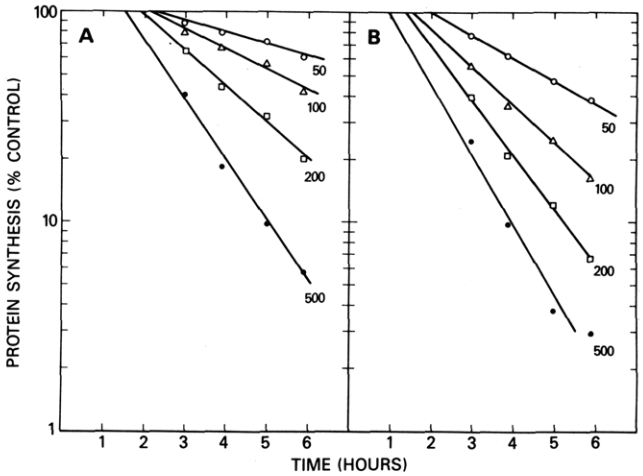

FIGURE 3: Kinetics of protein synthesis inhibition by OX7–ricin conjugates. Conjugates possessing either (A) one ricin per IgG or (B) a mixture of one and two ricins per IgG molecule were incubated at either 50, 100, 200, or 500 ng/mL with 10^5 AKR SL2 cells in leucine-free RPMI plus 100 mM lactose, 0.1% BSA, and 25 mM HEPES. At designated times [^{14}C]leucine was added. After a 1-h pulse, the extent of protein synthesis was determined (see Materials and Methods). The data points are represented at the midpoint of the 60-min incubation. Each data point represents the mean of quadruplicate values. Data were derived as cpm with a standard deviation equal to or less than 8% of the mean cpm for data in (A) and 11% in (B). Graphically, the points are presented as percent of control, which was generally 20 000 cpm.

200 000 band (calculated M_r 210 000) and a one to two ratio for the heavier band (calculated M_r 270 000). Native OX7 banded at M_r 150 000, and ricin at M_r 60 000. The lighter conjugate was designated IgG·R_1 and the preparation yielding two bands, IgG·R_{1+2}. This designation is used in the remainder of this paper. Densitometric scanning demonstrated a 33:67 distribution ratio of protein between the IgG·R_2 and IgG·R_1 bands, respectively, for the conjugate in lane 2. This implied that there is a 0.38:1.00 molar ratio of the biricin to monoricin conjugate and an average of 1.3 ricin molecules per immunoglobulin for the IgG·R_{1+2} preparation (discussed in fuller detail later). There was an apparent absence of heavier conjugates in these fractions and no immunoglobulin or ricin homopolymers; although, on freezing and thawing, lower molecular weight material appeared, including bands at the positions of free IgG and ricin.

Protein Synthesis Inhibition by Immunotoxins. A comparison of the toxicity of these two types of conjugates, the immunotoxins containing either one ricin (IgG·R_1) or a mixture of one and two ricins (IgG·R_{1+2}), was accomplished by incubating cells possessing the Thy-1.1 antigen, toward which the antibody is directed, in the presence of 100 mM lactose to minimize interaction of ricin with its cellular receptor. The inhibition of protein synthesis of AKR SL2 cells by the IgG·R_1 and IgG·R_{1+2} preparations at varying input concentrations is shown in panels A and B of Figure 3, respectively. It is apparent that the immunotoxin possessing, on the average, more than one ricin had greater cytotoxicity at any concentration. The IgG·R_{1+2} resulted in a shorter lag period, followed by a greater (pseudo-) first-order decline in protein synthesis.

In order to bring about a meaningful comparison of different types of conjugates, we found a need to develop a means of comparing kinetic data. We explored the relationship of input concentration of immunotoxin with the resultant slope on protein synthesis inhibition curves. In general, a kinetic examination of protein synthesis inhibition with most toxins results first in a lag period, followed by an exponential decline in protein synthesis. The (pseudo-) first-order decrease does

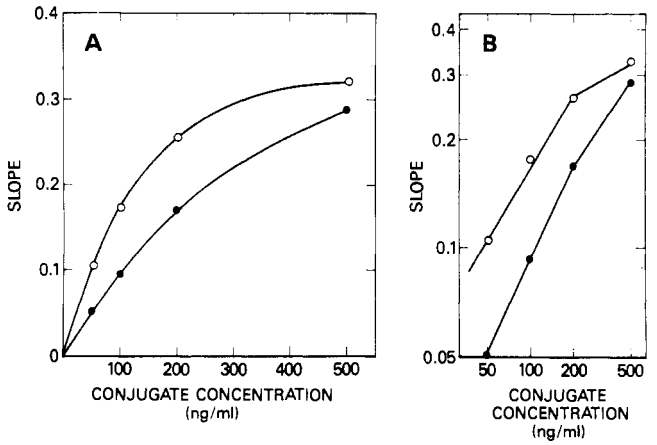

FIGURE 4: (A) Nonlinear relationship of rate of inhibition of protein synthesis and conjugate concentration. Plotting the positive value of the slopes from Figure 3 vs. the concentrations of the conjugates. Open circles, OX7 conjugate possessing a mixture of one and two ricins per immunoglobulin. Closed circles, one ricin per immunoglobulin. (B) Comparison of two types of conjugates on a log–log plot. Positive values of the slopes derived from the data of this figure are plotted vs. conjugate concentration. Open circles, OX7 conjugate possessing one and two ricins per immunoglobulin. Power function curve fitting ($y = ax^b$): $a = 0.0088$, $b = 0.64$, $R^2 = 0.99$ for concentration range of 50–200 ng/mL. Closed circles, one ricin per immunoglobulin. Power function curve fitting: $a = 0.0028$, $b = 0.75$, $R^2 = 0.99$.

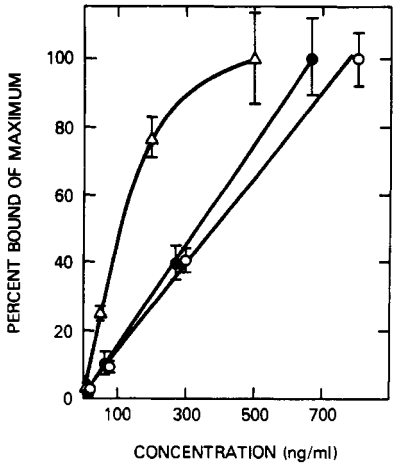

FIGURE 5: Steady-state binding of labeled antibody and conjugates to target cells. AKR SL2 cells were preincubated in RPMI, 0.1% BSA, 100 mM lactose plus 25 mM 2-deoxyglucose, and 5 mM azide at 37 °C for 30 min, followed by the addition of varied concentrations of labeled protein: antibody (OX7, 2000 Ci/mmol), triangles; monoricin conjugate (IgG·R_1, 1900 Ci/mmol), filled circles; mixed mono- and biricin conjugate (IgG·R_{1+2}, 3100 Ci/mmol), open circles. Additions, given in nanograms per milliliter for the two conjugates were corrected to yield approximate equal molar values when compared to the OX7 antibody inputs. After 30 min, bound material was determined as described under Materials and Methods. All values are plotted as the mean value of triplicate determinations ± standard deviation and have been normalized to the maximum cpm bound for that species. Nonspecific binding (which has not been substrated here) at 10^{-10} M for the OX7 label was 0.2% of total label; IgG·R_1, 0.2%; IgG·R_{1+2}, 1.6%. At 10^{-10} M labeled antibody became 35.8 ± 3.2% (of total bound; IgG·R_1, 13.1 ± 0.8%; IgG·R_{1+2}, 12.1 ± 0.7%.

not begin immediately as the first inhibition is detected. When enough data points are taken, there appears to be some curvature early in the process (Esworthy & Neville, 1984). For that reason, we have utilized data only within the linear portion of the inhibition curves. When the slopes of the protein synthesis curves for the various concentrations of the conjugates (Figure 3) were plotted linearly vs. input concentration of the conjugates, a nonlinear relationship for both conjugates could be seen (Figure 4A). The slopes, or first-order rates of protein synthesis inhibition, have had their signs changed to positive values and are expressed in the units of logs per hour (Esworthy & Neville, 1984). The curves were found to fit well with the power function $y = ax^b$, where y is the slope of inactivation and x is the input concentration. The fit for IgG·R_1 conjugate, $a = 0.0028$ and $b = 0.75$, was good, with a coefficient of determination (R^2) of 0.99. This power function can be made linear by logarithms: log (slope of inactivation) = log a + b log (input concentration), and the resulting log–log plot for IgG·R_1 can be seen in Figure 4B (closed circles). A similar analysis from the data in Figure 4A was done for the IgG·R_{1+2} conjugate. The fit to a power function of this conjugate (Figure 4B, open circles) was excellent only if the data for the 500 mg/mL level were excluded ($R^2 = 0.99$ for 50–200 ng/mL).

It appears that some flattening of the two functions occurs at the higher input levels, although it is considerably more pronounced with the IgG·R_{1+2} conjugate. To determine if this flattening was due to saturation of the cellular binding sites, we examined the binding of radiolabeled conjugates to the target cells. This result (see Figure 5) suggested that the binding of the conjugates does not demonstrate any saturation of the cellular binding sites at the concentrations examined. As should be expected, the labeled antibody (Figure 5, triangles) does saturate the cellular sites. Assuming an equal distribution of label between bound and unbound OX7, approximately 4×10^{10} molecules of antibody have been bound by 5×10^4 cells, suggesting 8×10^5 Thy-1.1 sites/cell. This is similar to the number found on AKR mouse thymocytes (6×10^5 sites/cell; Mason & Williams, 1980), and in agreement with the estimate of 10^6 sites/cell given previously for the AKR SL2 cell (Badger et al., 1985).

What is suggested by the data in Figure 5 is that some aspect of the conjugation procedure has diminished the binding capacity of both conjugates; because of the stoichiometric binding of the conjugates (OX7 binding also appears stoichiometric at low input levels), the binding affinity does not appear to have been significantly decreased. At 10^{-10} M (15 ng/mL) 36% (see legend to Figure 5) of the labeled OX7 became bound. For comparison, 13% of the IgG·R_1 and 12% of the IgG·R_{1+2} became bound at the same input concentrations; this percentage was constant for the conjugates at the various concentrations examined. Two points should be made about the experiment in Figure 5: (1) The binding conditions used should not be considered at equilibrium. The conjugate concentrations are not held constant. The conditions are identical with those of the bioassay (as in Figure 3), which, out of necessity in doing large numbers of individual determinations, require small volumes and an adequate number of cells to accurately measure protein synthesis. (2) There is evidence that binding goes to near completion. AKR cells (10^5) were incubated with $\sim 10^{-11}$ M label in the presence of metabolic inhibitors plus 100 mM lactose in either 50 μL total volume or 100 μL total volume (twice the total label, but the same number of cells), and the counts bound at steady state were determined. When the label was OX7 antibody, the 50-μL samples of 10^5 cells (2×10^6/mL) bound 4212 ± 696 (mean value of triplicate determination ± standard deviation) cpm; the 100-μL samples (10^6 cells/mL) bound 9209 ± 876 cpm. A similar finding was found with the OX7·R_{1+2} conjugate (OX7·R_1 was not done): the 50-μL sample bound 1687 ± 424 cmp, and the 100-μL sample bound 3148 ± 612 cpm. These results suggest two features. First, not all of the label is capable of binding. It is possible the iodination procedure damaged the protein. Second, at low antibody or conjugate

levels the cells are essentially depleting the medium of "bindable" label. The decrease in binding for the conjugates (compared to native antibody) may be due to the chemical activation procedures used to couple the antibody to ricin, steric hindrance of the antibody binding site, and/or a differential inactivation by the iodination. However, a similar binding capacity of the two conjugates would not necessarily be expected under these conditions.

The deviations from linearity at high conjugate concentrations do not lessen the value of the power function plot (Figure 4). The plot does permit a direct comparison of two conjugates. By comparing the concentrations of two conjugates required to reach similar inactivation rates (equal slope values on the ordinate), one derives the potency differential of the two conjugates, whereas the differences in rate of protein synthesis inhibition at similar input values (abscissa) yield a comparison in efficacy. Although we have plotted mass units on the abscissa, since this is the most accurate measurement of input for conjugates containing mixed species, estimates for conjugate molarity or ricin molarity can be easily superimposed. Under conditions where binding is not stoichiometric such as would be the case for low-affinity antibodies, receptor occupancy should be plotted on the x axis (Esworthy & Neville, 1984). Potency and efficacy are not as easily obtained with dose–response (or titration) curves. In the presence of stoichiometric binding, the hyperbolic nature of Figure 4A suggests that the (pseudo-) first-order rate-limiting process is saturable. This feature is also evident in the power function plot (Figure 4B). The potency differential of the conjugates varies with concentration, and at high conjugate concentrations both curves approach similar values. To reach a 0.5 log/h protein synthesis inhibition rate, one needs 2.05 times higher concentration of IgG·R_1 than IgG·R_{1+2}. In that a pure IgG·R_2 would represent less than a 50% increase in ricin per nanogram of conjugate over pure IgG·R_1, and in that the more toxic conjugate in Figure 4B does possess a significant level of IgG·R_1, it would appear that the toxicity of these conjugates is somehow potentiated by the addition of a second ricin molecule.

Densitometric readings (see Materials and Methods) of lane 2 in Figure 2 indicated that the protein distribution was 33% IgG·R_2 and 67% IgG·R_1 (calculated M_r 270000 and 210000, respectively) resulting in an average 1.3 ricins per IgG molecule and an average molecular weight of 230000. Thus, by mass, IgG·R_1 is 29% ricin, and the IgG·R_{1+2} species can be estimated to be 36% ricin. The 2.05 mass input differential (to reach similar inhibition rates) implies that you need 1.86 times more moles of IgG·R_1 than IgG·R_{1+2} (defined here as a single species of M_r 230000) and thus 1.4 times more ricin.

In light of the above finding, an additional preparation of conjugates was accomplished with isolation of smaller fractions. Two fractions were demonstrated on acrylamide gel to be predominantly IgG·R_2 and IgG·R_3 (Figure 6). These conjugates were incubated with AKR cells, and the resultant loss of protein synthesis for conjugate concentrations of 200 ng/mL is shown in Figure 7. Although the production yields were too low to undertake any extensive analysis, these two isolated conjugates, IgG·R_2 and IgG·R_3, were obviously quite different in cytotoxicity. The IgG·R_1, which is identical with the material examined earlier, yielded a 0.14 log/h inhibition rate. IgG·R_2 resulted in 0.43 log/h and IgG·R_3 in 0.20 log/h. The high toxicity of the IgG·R_2 further suggests the presence of potentiation of cytotoxicity when the conjugate possesses two ricins per immunoglobulin. The failure of the IgG·R_3 to have even greater toxicity may be due to steric hindrance with

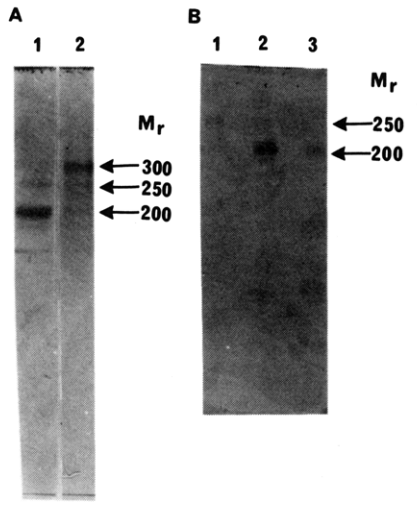

FIGURE 6: Acrylamide gradient electrophoresis gel of OX7–ricin conjugates. The two gels were run as described in Figure 2. (A) Ricin–antibody conjugate containing three ricins per immunoglobulin (lane 2, band at M_r 300000), compared to a monoricin conjugate (lane 1). Protein application to lane 2 was 3.5 μg. (B) Ricin–antibody conjugate containing two ricins per immunoglobulin (lane 1, 0.2 μg applied). The samples were acquired from fractions off a gel filtration column. For comparative purposes, two other fractions are shown in lane 2 (mixture of mono- and biricin conjugate) and lane 3 (monoricin conjugate).

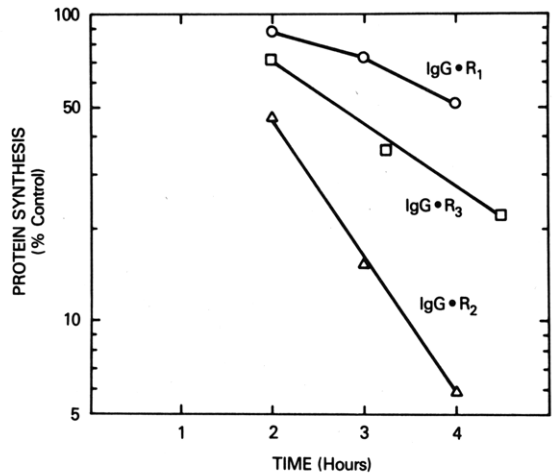

FIGURE 7: Kinetics of protein synthesis inhibition by OX7–ricin conjugates. Three types of conjugates, possessing either one ricin (circles), two ricins (triangle), or three (squares) per immunoglobulin, all at 200 ng/mL, were compared in their ability to inhibit protein synthesis in AKR SL2 cells in the presence of 100 mM lactose as described in the legend of Figure 3. All data points represent quadruplicate determinations with a standard deviation of 12% or less of the mean cpm values. Molecular weights of mono-, bi-, and triricin conjugate can be calculated to be 21000, 270000, and 330000, so that 200 ng/mL solutions would be 0.95, 0.74, and 0.67 nM. The IgG·R_{1+2} species would be 0.24 nM in the biricin and 0.64 nM in the monoricin conjugate (calculated from the estimated 33%:67% distribution in protein between the biricin and monoricin species).

decreases in both antibody– and ricin–membrane interactions. The increase in cytotoxicity for the IgG·R_2 species, over the IgG·R_{1+2} (0.30 log/h; data not shown), implies that the potentiation in going from one to two ricins per immunoglobulin is even greater than the 2.05 factor derived above. If one views the IgG·R_{1+2} as a mixture and ascribes the 2.05 potency gain strictly to the IgG·R_2 species present (33% total protein), then this species on a mass scale is 6.2 times more potent than the IgG·R_1 conjugate (and 8.0 times more potent on a conjugate molar scale).

The remarkable potentiation of cytotoxicity seen through the addition of a second ricin might be interpreted as a result

of increased binding due to the divalency of the ricin with a resultant increased affinity. Interaction of the ricin moiety with its membrane receptor would be increased for the conjugate even in the presence of lactose, once bound to the cell surface through the antibody moiety. However, labeled OX7 antibody preincubated (at 150 ng/mL) with AKR cells, as in Figure 5, and then diluted 100-fold into fresh medium (containing 25 mM 2-deoxyglucose, 5 mM azide, and 100 mM lactose) resulted in no measurable dissociation over a 2-h period at 37 °C. The IgG·R_{1+2} conjugate at the same concentration also displayed no dissociation (data not shown). Thus, under the normal conditions of the protein synthesis assays, the antibody binding is essentially irreversible, so that further increases in affinity alone would not be expected to result in increased toxicity. We cannot exclude at this time the possibility that the ricin moiety interacts with cellular receptors once the conjugate becomes firmly bound. Indeed, we entertain the thought that once the conjugate is internalized and the lactose is transported out of the endosome (Besterman et al., 1981), ricin–membrane interactions take place that are essential for conjugate toxicity. The intravesicular membrane binding of the conjugate through the ricin moiety may be essential for the proper routing of the ricin conjugate.

Although previous works with unfractionated conjugates have suggested that ricin–antibody conjugates and ricin toxin do not appear to gain entry to the cytosol through identical processes (Youle & Neville, 1982; Esworthy & Neville, 1984), the various conjugates may utilize, to varying degrees, the toxin's normal efficient entry route. What is very apparent with these conjugates is the presence of a lag period (see Figure 3). The extrapolation of the linear portion of the curves to the x axis results in lag periods that are, like ricin, related inversely with concentration. The exceptional effect of ricin number per immunoglobulin on toxicity and the relationships of conjugate concentration with the inactivation rates and lag periods suggest a functional importance of the ricin moiety in the rate-limiting step of the conjugate intoxication process.

The variables involved in immunotoxin construction and their effect on cytotoxicity have received minimal attention. Optimization of the functional aspects of conjugates will require an understanding of what these variables are. This report describes the effects that the number of ricins per immunoglobulin have on the conjugates' potency. In addition is the finding that conjugation may reduce the antibodies binding capacity.

ACKNOWLEDGMENTS

We acknowledge the excellent technical assistance of Mary Alice G. Kimak and James M. Boone. We thank Sandra Means and Pamela McKinley for preparation of the manuscript.

Registry No. Thy, 65-71-4.

REFERENCES

Badger, C. C., Krohn, K. A., Peterson, A. V., Shulman, H., & Bernstein, I. D. (1985) *Cancer Res. 45*, 1536–1544.

Baenziger, J., & Fiete, D. (1979) *J. Biol. Chem. 254*, 9795–9799.

Besterman, J. M., Airhart, J. A., Woodworth, R. C., & Low, R. B. (1981) *J. Cell Biol. 91*, 716–727.

Ellman, G. L. (1959) *Arch. Biochem. Biophys. 82*, 70–77.

Esworthy, R., & Neville, D. M., Jr. (1984) *J. Biol. Chem. 259*, 11496–11504.

Fairbanks, G., Steck, T., & Wallach, D. (1971) *Biochemistry 10*, 2606–2617.

Gilliland, D., Steplewski, Z., Collier, J., Mitchell, K., Chang, T., & Koprowski, H. (1980) *Proc. Natl. Acad. Sci. U.S.A. 77*, 4539–4543.

King, T., Li, Y., & Kochoumian, L. (1978) *Biochemistry 17*, 1499–1506.

Kitagawa, T., & Aikawa, T. (1976) *J. Biochem. (Tokyo) 79*, 233–236.

Krolick, K. A., Villemex, C., Isakson, P., Uhr, J., & Vitetta, E. (1980) *Proc. Natl. Acad. Sci. U.S.A. 77*, 5419–5423.

Liu, F.-T., Zinnecker, M., Hamaoka, T., & Katz, D. (1979) *Biochemistry 18*, 690–697.

Mason, D. W., & Williams, A. F. (1980) *Biochem. J. 187*, 1–20.

Morrison, M. (1980) *Methods Enzymol. 70*, 214–220.

Neville, D. M., Jr. (1985) in *Directed Drug Delivery* (Borchardt, R., Repta, A., & Stella, V., Eds.) pp 211–230, Humana, Clifton, NJ.

Olsnes, S., Refsnes, K., & Pihl, A. (1974) *Nature (London) 249*, 627–631.

Schramm, H., & Pülffer, T. (1977) *Z. Physiol. Chem. 358*, 137–139.

Thorpe, P. E., Ross, W. C. J., Brown, A. N. F., Myers, C. D., Cumber, A. J., Foxwell, B. M. J., & Forrester, J. T. (1984) *Eur. J. Biochem. 140*, 63–71.

Traut, R., Bollen, A., Sun, T.-T., Hershey, J., Sundberg, J., & Pierce, L. (1973) *Biochemistry 12*, 3266–3273.

Youle, R. J., & Neville, D. M., Jr. (1980) *Proc. Natl. Acad. Sci. U.S.A. 77*, 5483–5486.

Youle, R. J., & Neville, D. M., Jr. (1982) *J. Biol. Chem. 257*, 1598–1601.

Youle, R. J., Murray, G. J., & Neville, D. M., Jr. (1981) *Cell (Cambridge, Mass.) 23*, 551–559.